

2023

## Stability Chart of Generalized Bessel Equation

Mohamed Elborhamy

Follow this and additional works at: <https://digitalcommons.aaru.edu.jo/erjeng>

---

### Recommended Citation

Elborhamy, Mohamed (2023) "Stability Chart of Generalized Bessel Equation," *Journal of Engineering Research*: Vol. 7: Iss. 3, Article 19.

Available at: <https://digitalcommons.aaru.edu.jo/erjeng/vol7/iss3/19>

This Article is brought to you for free and open access by Arab Journals Platform. It has been accepted for inclusion in Journal of Engineering Research by an authorized editor. The journal is hosted on [Digital Commons](#), an Elsevier platform. For more information, please contact [rakan@aar.edu.jo](mailto:rakan@aar.edu.jo), [marah@aar.edu.jo](mailto:marah@aar.edu.jo), [u.murad@aar.edu.jo](mailto:u.murad@aar.edu.jo).

# Stability Chart of Generalized Bessel Equation

Mohamed El-Borhamy<sup>1</sup>

<sup>1</sup>Department of Engineering Mathematics and Physics, Faculty of Engineering, University of Tanta 31527, Egypt. – email: mohamed.elborhamy@f-eng.tanta.edu.eg

<sup>1</sup>Department of Basic Sciences, Faculty of Engineering, Horus University, New Damietta, Egypt. – email: mborhamy@horus.edu.eg

**Abstract-** In this article, it is aimed to look for a semi-analytical relation between the eigenvalue and the order of generalized Bessel differential equation using the asymptotic iteration and perturbation methods. Based on the analytical results, the stability chart between the eigenvalue and the order of the equation is constructed. Accordingly, through the path of verification and investigation by using the numerical results with Fourier spectral method, a strong fit with the analytical results is observed.

**Keywords-** Stability chart; Bessel equation; Asymptotic iteration method (AIM); Perturbation methods.

## I. INTRODUCTION

The stability or boundedness of solutions of such linear systems with periodic coefficients has been extensively studied and characterized in terms of eigenvalue curves that demarcate the boundaries of stability and instability regions. In these systems, it has typically become the drawing of the so-called stability chart or Ince-Strutt diagram, which based on a relationship among the parameters of the system, is indispensable in the stability analysis, cf. [25,35,40].

Stability charts or Ince-Strutt diagrams represent a very attractive way to construct a diagram for the linear periodic systems to predict the domains of stability and their boundaries or the transition curves. These boundaries consist of one-dimensional curves in the space of system parameters that separate points for which at least one solution is unbounded (unstable) from points for which all solutions are bounded (stable). Since, the main criterion to specify transition curves or stability boundaries is the solutions remain bounded in the course of time or grow indefinitely. Typically, there are various algorithms and numerical schemes are created to draw the stability charts for the undamped/damped linear periodic systems, cf. [18,20,21].

Some workers in the field are suggested some analytical expressions to express the stability boundaries in contrast to the numerical schemes, cf. [9,22,32,34,37,42]. With a large number of different solution algorithms available, it is needed to note that for specific eigenvalue problems, there is no single algorithm which can be employed to provide an efficient process to construct stability charts, cf. [24,36,39]. However, the variation of eigenvalue is always associated with the inherited parameters in the dynamic problems.

In any case, to configure the main idea behind in the introduced work, it is necessary to present in our introduction some examples of dynamical systems with periodic coefficients for which stability charts have been constructed. Actually, these charts have become the key

factors in the study of the stability analysis for these systems. The introduced systems are represented by three equations used in the celebrated engineering and scientific applications, namely, Mathieu equation, Ince equation and El Borhamy-Rashad-Sobhy equation.

### 1.1 Mathieu equation

Mathieu equation represents the first example for the construction of the stability chart that is introduced by Ince in [23]. Mathieu equation was first introduced by E'mile L'eonard Mathieu, who encountered it while studying vibrating elliptical drumheads, cf. [29]. The importance of Mathieu equation lies in its possession of vast applications in physical and engineering sciences, cf. [8,30,41]. However, the general damped form of Mathieu equation reads

$$y''(x) + 2\zeta y'(x) + (\lambda - 2v \cos 2x)y(x) = 0, \quad (1)$$

where  $\zeta$  is the damping coefficient,  $\lambda$  is the eigenvalue parameter and  $v$  is the internal forcing(exciting) amplitude.

In fact, the analytical solution of the general Mathieu equation has not found yet. The mathematical treatment only is reduced to create a numerical algorithm to obtain the numerical solution which is typically inconveniently for the practical use of Mathieu equation.

Indeed, there are in the cases of physical applications which the analytical dependencies are required to understand the associated physical processes with the corresponding problem parameters.

Let us first recognize the stability chart of the undamped equation which called angular Mathieu equation(AME). The AME reads

$$y''(x) + (\lambda - 2v \cos 2x)y(x) = 0. \quad (2)$$

The undamped AME is a second order linear differential equation that has two families of independent periodic solutions, namely the even and the odd angular Mathieu functions(i.e.  $ce_n$  and  $se_n$ ). This notation of 'ce' and 'se' comes from cosine-elliptic and sine-elliptic, since it is a widely accepted notation for angular Mathieu function. The mathematical properties such as parity, periodicity, and normalization of the AMF are exactly the same as their trigonometric counterparts of cosine and sine functions. That is,  $ce_n$  is even and  $se_n$  is odd, and they have period  $\pi$  when  $n$  is even or period  $2\pi$  when  $n$  is odd. The AMF have  $n$  real zeros in the open interval  $(0, \pi)$ , but they cluster around  $\pi/2$



as  $\nu$  increases. The range of the plots has been limited to  $(0, \pi)$ , because their entire behavior can be concluded from the parity and symmetry relations. So, the general solution  $\mathcal{Y}(x)$  of Eq.(2) is written as

$$\mathcal{Y}(x) = C_1 y_1(x) + C_2 y_2(x), \quad (3)$$

where,  $C_1$  and  $C_2$  are arbitrary constants.

According to Floquet theory, there always exists a solution of Eq.(2) in the form say  $\mathcal{Y}_1(z) = e^{i\mu x} P(x)$  where  $\mu$  is the characteristic exponent which depends on the main parameters  $\lambda$  and  $\nu$ . Also, the function  $P(x)$  is a periodic function with the minimal period  $(\pi)$ . The two solution of  $\mathcal{Y}_1(x)$  and  $\mathcal{Y}_2(x)$  have different behaviors according to the values of  $\mu$ , for details, cf. [14].

Typically, in case to obtain periodic solutions with period  $\pi$  or  $2\pi$ , then the two parameters  $\lambda$  and  $\nu$  must satisfy the equation  $\mu(\lambda, \nu) = n$ , where  $n$  is an integer number and all eigenvalues ( $\lambda$ ) are called characteristic values. So, the corresponding periodic solutions  $\mathcal{Y}_1(x)$  are always called Mathieu functions of the first kind but the second solution  $\mathcal{Y}_2(x)$  (Mathieu function of the second kind) is normally rejected due to its unboundedness.

It is easy to deduce that if  $\mu(\lambda, \nu) = n$ , then  $\mathcal{Y}_1(x)$  is periodic with period  $\pi$  for even  $n$  and periodic with period  $2\pi$  for odd  $n$ . So, the solution  $\mathcal{Y}_1(x)$  can be represented by the following Fourier expansion,

$$\mathcal{Y}_1(x) = \sum_{n=0}^{\infty} (A_n \cos nx + B_n \sin nx). \quad (4)$$

Then, by using the harmonic balance method, it might be to obtain recurrence relations for the coefficients  $A_n$  and  $B_n$  based on  $\lambda$  and  $\nu$  parameters.

Because the angular Mathieu functions  $ce_n$  and  $se_n$  are periodic with period  $\pi$  or  $2\pi$ , then they can be expanded in terms of Fourier series. The corresponding expansions fall into four classes according to symmetry and anti-symmetry about  $x = 0$  or  $x = \pi/2$  and read

$$ce_{2m}(x, \nu) = \sum_{n=1}^{\infty} A_{2n}^{(2m)}(\nu) \cos 2nx, \quad (5a)$$

$$ce_{2m+1}(x, \nu) = \sum_{n=1}^{\infty} A_{2n+1}^{(2m+1)}(\nu) \cos(2n + 1)x, \quad (5b)$$

$$se_{2m+2}(x, \nu) = \sum_{n=0}^{\infty} B_{2n+2}^{(2m+2)}(\nu) \sin(2n + 2)x, \quad (5c)$$

$$se_{2m+1}(x, \nu) = \sum_{n=0}^{\infty} B_{2n+1}^{(2m+1)}(\nu) \sin(2n + 1)x, \quad (5d)$$

where  $m = 0, 1, 2, \dots$ . The recurrence relations between the coefficients can be concluded by substituting these series (Eq.5) in the angular Mathieu equation (Eq.(2)) to obtain

$$|H - \lambda I| = 0 \quad (6)$$

where  $H$  is the symmetric matrix (Hill's matrix). Eq.(6) represents the equation of eigenvalues of  $H$ , for which the linear system has non trivial solution. Hence, all obtained eigenvalues are functions in terms of  $(\nu)$ . Typically, if  $\nu$  is real then  $H$  is real symmetric and all the eigenvalues are real.

By considering that, the values of  $a_m$  and  $b_m$ , that satisfy the condition of Eq.(2), are the eigenvalues of the equation for  $ce_m$  and  $se_m$  respectively. According to the Sturm-Liouville theory, the eigenvalues form an infinite set of countable real values that have an ordered property. Each function  $ce_m$  and  $se_m$  is associated with an eigenvalue  $a_m$  and  $b_m$  which in turn depends on  $\nu$  respectively. Usually, they can be placed in ascending order as follows:

$$a_0 < a_1 < b_1 < b_2 < a_2 < a_3 < b_3 < \dots \text{ if } \nu < 0. \quad (7)$$

and

$$a_0 < b_1 < a_1 < b_2 < a_2 < b_3 < a_3 < \dots \text{ if } \nu \geq 0. \quad (8)$$

In particular, notice that when  $\nu = 0$  one has  $a_0 = 0$  and  $a_m = b_m = m^2$ . Now yet, the angular Mathieu functions obtained are defined as  $ce_m(x, \nu)$  (even solutions corresponding to  $a_m$  eigenvalues) and  $se_m(x, \nu)$  (odd solutions corresponding to  $b_m$  eigenvalues).

Note that, Eq.(2) becomes the harmonic equation when  $\nu = 0$ , when it is evident that  $ce_m$  and  $se_m$  become equal to the trigonometric functions  $\cos mx$  and  $\sin mx$  as  $\nu$  vanishes.

Let us seek the solutions with Mathieu functions  $ce_m(x, \nu)$  and  $se_m(x, \nu)$  for nonzero  $\nu$  in the following form:

$$ce_m(x, \nu) = \cos mx + \sum_{n=1}^{\infty} \nu^n c_n(x), \quad (9a)$$

$$se_m(x, \nu) = \sin mx + \sum_{n=1}^{\infty} \nu^n s_n(x), \quad (9b)$$

$$\lambda = m^2 + \sum_{n=1}^{\infty} \alpha_n \nu^n. \quad (9c)$$

The constants  $\alpha_n$ ,  $c_n(x)$  and  $s_n(x)$  should be determined by substituting equations of Eq.(9) into equation Eq.(2).

Then, a complete solution therefore is of the form:

$$\mathcal{Y}(x) = C_3 ce_m(x, \nu) + C_4 se_m(x, \nu), \quad (10)$$

where  $C_3$  and  $C_4$  are arbitrary real constants. In an analogous manner of harmonic balance method, a complete

hierarchy of periodic solutions of odd and even type can be established for  $ce_m(x, v)$  with  $m = 0, 1, 2$  as follows:

$$ce_0(x, v) = 1 - \frac{1}{2}v \cos 2x + \frac{1}{32}v^2 \cos 4x + \dots \quad (11a)$$

$$ce_1(x, v) = \cos x - \frac{1}{8}v \cos 3x + \frac{1}{64}v^2 \left( -\cos 3x + \frac{1}{3} \cos 5x \right) + \dots \quad (11b)$$

$$ce_2(x, v) = \cos 2x - \frac{1}{8}v \left( \frac{2}{3} \cos 4x - 2 \right) + \frac{1}{384}v^2 \cos 6x + \dots \quad (11c)$$

In a similar manner, the function  $se_m(x, v)$  can be established for with  $m = 1, 2$  as follows:

$$se_1(x, v) = \sin x - \frac{1}{8}v \cos 3x + \frac{1}{64}v^2 \left( \sin 3x + \frac{1}{3} \cos 5x \right) + \dots \quad (12a)$$

$$se_2(x, v) = \sin 2x - \frac{8}{12}v \sin 4x + \frac{1}{384} \sin 6x + \dots \quad (12b)$$

and so on, with the corresponding eigenvalues or the characteristic numbers read,

$$a_0: \lambda = -\frac{1}{2}v^2 + \frac{7}{128}v^4 - \frac{29}{2304}v^6 + \dots \quad (13a)$$

$$a_1: \lambda = 1 + v - \frac{1}{8}v^2 - \frac{1}{64}v^3 + \dots \quad (13b)$$

$$b_1: \lambda = 1 - v - \frac{1}{8}v^2 + \frac{1}{64}v^3 - \dots \quad (13c)$$

$$a_2: \lambda = 4 + \frac{5}{12}v^2 - \frac{763}{13824}v^4 + \dots \quad (13d)$$

$$b_2: \lambda = 4 - \frac{1}{12}v^2 + \frac{5}{13824}v^4 - \dots \quad (13e)$$

From Eq.(13), it can be obtained pairs of  $\lambda$  and  $v$  that satisfy the characteristic numbers used in creating an approximate stability chart for the Mathieu equation.

Typically, the eigenvalue curves in Mathieu equation arise from  $\pi$  and  $2\pi$  periodic solutions. Hence, these periodic solutions are not finite as shown in Eq.(11), Eq.(12) and Eq.(13). In general, it is a way to obtain the transition curves by truncating the series solution of Mathieu functions.

Here, the curves are drawn with ten terms used as shown in Fig.1 and Fig.2. As vividly shown, the curves divide the  $(\lambda, v)$  domain into parts or regions where the solutions of the (un)damped equations are stable or unstable separated by the transition curves representing the curves of Eq.(13).

As shown in Fig.1, the curves denote the characteristic curves for even and odd of both  $ce_m(x, v)$  and  $se_m(x, v)$

Mathieu functions. Hence, even and odd orders curves of  $ce_m(x, v)$  and  $se_m(x, v)$  are symmetrical and anti-symmetrical about the  $\lambda$ -axis, respectively. Thus, they divide the  $(\lambda, v)$  plane in regions where the solutions of the undamped equation are periodic, stable or unstable. It is clearly that, the unstable regions touch the axis  $v = 0$  at values  $\lambda = m^2$ .

In the damped Mathieu equation, the eigenvalues of the system shown in Fig.2 are easily found by Eq.(6), which gives a relation between  $\lambda$  and  $v$  that defines the transition curves for fixed values of  $\zeta$ .

If  $\zeta$  has a value then, the curves detached from the horizontal axis or  $\lambda$ -axis. Also, at most, the same detachment of the eigenvalue curves is also anticipated from the fractional order Mathieu equation definitely, when the fractional order is presented in the damped term as discussed in [18, 35].

Also, it is clear that, a slight change in the damping coefficient ( $\zeta$ ) affects the shape and location of eigenvalue curves. Such that, the effect can be noticed by the location of the minimum point on the transition curve, which is specified by the lowest value of the exciting amplitude ( $v$ ).

Indeed, the location of the minimum point on the eigenvalue curves due to the damping coefficient is moved in the vertical direction until the unstable regions are disappeared. In the other hand, in the case of fractional derivative of damping as in [18], the influence of fractional order parameter of the damping term moves this lowest point horizontally to the right direction. Typically, all these results are confirmed also in [35, 40].

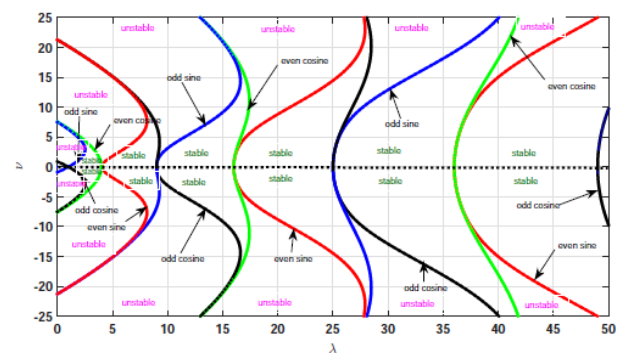


Figure 1. Stability chart and eigenvalue curves (transition curves) of un-damped Mathieu equation ( $\zeta = 0$ ).

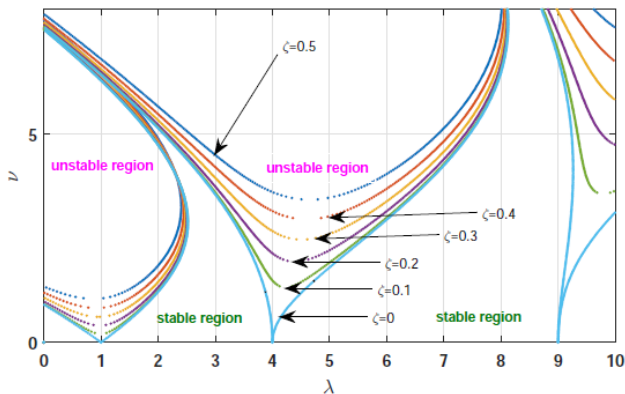


Figure 2. Stability chart and eigenvalue curves of damped Mathieu equation for different values of  $\zeta$ .

### 1.2 Ince equation

We take Ince equation as a second example used to describe numerous physical problems in the fields of applied sciences and engineering such as evolutionary game theory, vibrational mechanics and laser optics, cf. [13, 35, 23]. This equation reads.

$$y'' + (2\zeta + \epsilon \sin 2x) y' + (\lambda - \epsilon p \cos 2x) y = 0. \quad (14)$$

The difference between Mathieu and Ince equations is the last involves the forcing amplitude in the damping term too. But the mathematical treatment of Ince equation is quite similar of Mathieu equation and their periodic solutions can be formed by using Mathieu functions. The work on Ince equation also can be extended to obtain the results which are closely related Mathieu equation definitely if the damping term is neglected. The stability chart of Ince equation using  $\lambda - \epsilon$  plane can be shown in Fig.3.

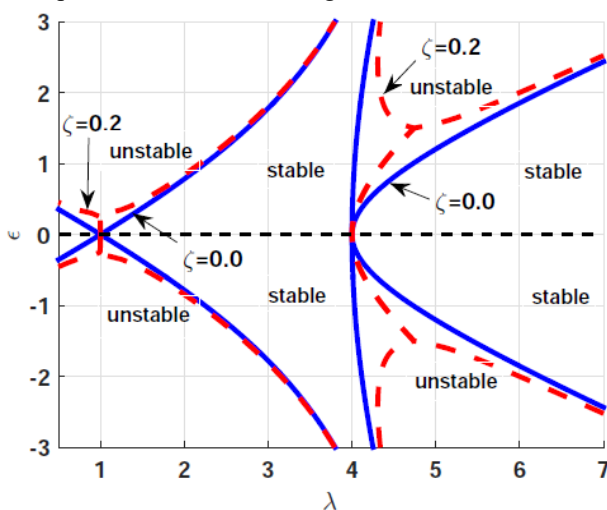


Figure 3. Stability chart and eigenvalue curves of Ince equation at  $p = 1.5$  and  $\zeta = 0$  and  $0.2$ .

### 1.3 El Borhamy-Rashad-Sobhy equation

As a third example, this equation is used to discuss the modeling of periodic responses for the dynamical motion of AC machines by using the representation of the equivalent linear RLC series circuit. It is considered into account the periodic variation of inductance to express the relative movement between the stator and rotator parts of the machine.

This leads to the existence of the eigenvalue parameter in the damped term which makes the equation is different from classical eigenvalue problems with periodic coefficients such as Mathieu and Ince equations. However, this equation reads

$$(1 + h \cos 2x) y'' + \frac{Q}{\alpha} y' + \frac{1}{\alpha^2} y = 0. \quad (15)$$

The stability chart is constructed  $(h, \alpha)$  plane in the presence of damping parameter  $Q$  explaining the stability and instability domains as clearly shown in Fig.4. The mathematical analysis of the model to obtain eigenvalue curves with various methods is discussed in [19].

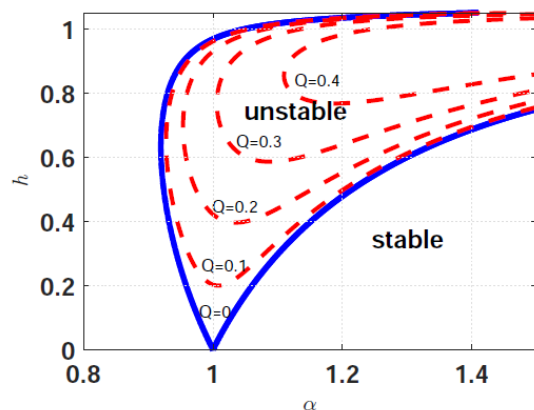


Figure 4. Stability chart and eigenvalue curves of El Borhamy-Rashad-Sobhy equation at different values of  $Q$ .

### 1.4 Aim of the work

In this work, it is aimed to predict the stability chart of a generalized Bessel equation as one of the modified form of Bessel equation, and it reads,

$$x^2 y'' + (2\zeta x + \gamma) y' + (\lambda x^2 + (1 - \delta)x - \nu^2) y = 0, \quad (16)$$

where  $\zeta, \gamma, \lambda, \nu$  and  $\delta$  real (or complex) constants within the domain  $x \in (a, b)$ .

Since, the classical Bessel differential equation and its modified forms as introduced in [3,26], the expression of their solutions might have a structure in terms of trigonometric functions definitely if its order is integer. Then, it is anticipated to obtain a predicted stability chart between  $\lambda$  and  $\nu$  parameters in both classical, modified and generalized forms.

An additional purpose of this work is to discuss the existence of stability domains and transition curves





represented by the relation between the parameters in boundary value problems with polynomial coefficients. Beside the used semi-analytical method to obtain the relation between  $\lambda$  and  $\nu$ , Fourier spectral method is exploited as the most efficient numerical techniques in use for the periodic domains to verify the stability chart for the given problem. The semi-analytical relations between  $\lambda$  and  $\nu$  is constructed by using the perturbation method and asymptotic iteration method (AIM). In addition to, the results can be applied in engineering applications such as for the buckling problem as special application of Bessel equation to calculate the critical load of a column under its own weight and the external forces. In the use of Fourier spectral method as a validation technique, the basic steps of the numerical algorithms are presented in [6], and the eigenvalue solution techniques are presented to follow the expositions in [6,10,17,33].

## II. GENERALIZED BESSEL EQUATION

In common, Bessel equation(B.E.) is considered one of the most interesting practical equation in applied sciences due to its appearance frequently in all mathematical physics applications and their solutions represented by the Bessel functions (B.F.).

This equation was derived by Friedrich Wilhelm Bessel (1784-1846), who studied disturbances in planetary motion, which led him to deduce asystematic analysis of solutions of that equation, cf. [4].

Recently, several applications of B.E. have been discovered in applied sciences and engineering such as optics, elasticity, diffusion and in many problems of potential theory, cf. [2,16,38,44]. Although, the B.F. represents the solutions of a second order differential equation, but in fact, but it has a very close connection to the first order differential equations through Riccati differential equation and some others.

The behavior of the first kind of Bessel function  $J_\nu(x)$  for the real values of  $x$  is well known in an infinite series. In fact, it is possible to obtain an asymptotic series for  $J_\nu(x)$  in terms of trigonometric functions definitely if  $\nu = n(n \in \mathbf{Z})$ . This expression contains an amplitude and a phase angle, whose calculation requires writing  $J_n(x)$  in terms of certain contour integrals in the complex plane to obtain their trigonometric structure, cf. [28]. However, some special cases are provided from Eq.(16), which are mostly studied in [7,27,43,44].

## III. TRIGONOMETRIC REPRESENTATION OF BESSEL FUNCTIONS

It is typically known that the Bessel functions when  $\nu = n$  have an oscillatory property in nature and resemble damped sinusoids. Although these Bessel functions are not strictly periodic.

Some works are concerned with obtaining of several trigonometric expansions that have been used to as alternating forms for specific problems in a closed form.

Also, some of the closed form approximations for expressing the Bessel functions are derived by using polynomial, trigonometric or exponential expansions, cf. [3,5,7,15,28].

The following expansions have been obtained by Jacobi, so that it is called.

Jacobi expansions. They gave a representations of a plane wave by cylindrical coordinates.

$$\cos(x \sin \theta) = J_0 + \sum_{n=1}^{\infty} 2(-1)^n J_{2n}(x) \cos 2n\theta, \quad (17)$$

$$\sin(x \sin \theta) = \sum_{n=1}^{\infty} 2(-1)^n J_{2n+1}(x) \cos(2n + 1)\theta. \quad (18)$$

This yields, for integer  $n$ , the following Bessel's integral

$$J_n(x) = \frac{1}{\pi} \int_0^\pi \cos(x \sin \phi - n\phi) d\phi. \quad (19)$$

As mentioned in [5], the deduced approximation for  $J_\nu(x)$  reads

$$\frac{1}{N} \sum_{r=1}^N e^{(ix \sin \frac{2\pi r}{N} - \frac{2\pi r n}{N})} = J_n(x) + \sum_{m=1}^{\infty} [(-1)^{mN-n} J_{mN-n}(x) + J_{mN+n}(x)] \quad (20)$$

As an example, for  $N = 12$  and  $n = 0$ , one gets

$$\frac{1}{6} + \frac{1}{3} \cos \frac{x}{2} + \frac{1}{3} \cos \frac{\sqrt{3}x}{2} + \frac{1}{6} \cos x + \dots = J_0(x) + 2J_{12}(x) + 2J_{24}(x) + \dots \quad (21)$$

Although the approximations given by Eq.(21) deteriorate as  $n$  increases with improve greatly when  $n$  reaches the value of  $\frac{N}{2}$ . If  $N$  is a multiple of 4, within something of the orders, it can be obtained some trigonometric approximations as closely as the real values of  $J_n(x)$ ,  $n = 0, 1, 2, 3, 4, \dots$  with the aid of the following identities of Bessel functions,

$$J_1(x) = -\frac{d}{dx} J_0(x), \quad Y_1(x) = -\frac{d}{dx} Y_0(x) \quad (22a)$$

$$J_{n+1}(x) = J_{n-1}(x) - 2 \frac{d}{dx} J_n(x), \quad Y_{n+1}(x) = Y_{n-1}(x) - 2 \frac{d}{dx} Y_n(x) \quad (22b)$$

The calculation of higher order of Bessel functions can easily be deduced by using the approximation of  $J_0(x)$  in [45] for  $0 \leq x < 1$ ,

$$J_0(x) \approx \frac{1}{2} \cos\left(x \sin \frac{\pi}{8}\right) + \frac{1}{2} \cos\left(x \cos \frac{\pi}{8}\right), \quad (23)$$

Alternatively, or  $J_0(x)$  can be used for  $0 \leq x < 1$ , with the deduced identity in [5],

$$J_0(x) \approx \frac{1}{6} + \frac{1}{3} \cos \frac{x}{2} + \frac{1}{3} \cos \frac{3x}{2} + \frac{1}{6} \cos x. \quad (24)$$

Using the identities Eq.(22) and Eq.(24), it is easily to get for  $\lambda = 1$  and  $\nu = n = 1, 2, 3, 4$  the following approximations:

$$J_1(x) \approx \frac{1}{6} \sin \frac{x}{2} + \frac{\sqrt{3}}{6} \sin \frac{\sqrt{3}x}{2} + \frac{1}{6} \sin x, \quad (25a)$$

$$J_2(x) \approx \frac{1}{6} + \frac{1}{6} \cos \frac{x}{2} - \frac{1}{6} \cos \frac{\sqrt{3}x}{2} - \cos \frac{x}{6}, \quad (25b)$$

$$J_3(x) \approx \frac{1}{3} \sin \frac{x}{2} - \frac{1}{6} \sin x, \quad (25c)$$

$$J_4(x) \approx \frac{1}{6} - \frac{1}{6} \cos \frac{x}{2} - \frac{1}{6} \cos \frac{\sqrt{3}x}{2} + \frac{1}{6} \cos x \quad (25d)$$

which approved their validity up to a certain order of approximation in [1].

Accordingly, as a result Bessel functions of the first and second kinds, they can be approximated by using the structure of trigonometric Fourier series as follows:

$$J_{2n}(x) = \sum_{r=0}^{\infty} A_r^{(2n)} \cos \tau_r^{2n} x, \quad J_{2n+1}(x) = \sum_{r=0}^{\infty} B_r^{(2n+1)} \sin \tau_r^{2n+1} x, \quad (26a)$$

$$Y_{2n}(x) = J_{2n}(x) \int \frac{dx}{x J_{2n}^2(x)}, \quad Y_{2n+1}(x) = J_{2n+1}(x) \int \frac{dx}{x J_{2n+1}^2(x)} \quad (26b)$$

Hence, from the structure, it yields the existence of the eigenvalue curves in  $(\lambda, \nu)$  plane which divides the domain into stable and unstable regions.

#### IV. AIM SOLUTION OF THE GENERALIZED BESSEL EQUATION

Let us firstly give a brief review for the asymptotic iteration method (AIM) regarding the solution of 2nd order D.E.

$$y'' = q_0(x, \varepsilon)y' + s_0(x, \varepsilon)y, \quad (27)$$

where  $q_0(x, \varepsilon)$  and  $s_0(x, \varepsilon)$  are  $C^\infty$  functions and  $\varepsilon$  is a perturbation parameter. So that the  $n$ th derivative of the equation reads

$$y^{(n+2)} = q_n(x, \varepsilon)y' + s_n(x, \varepsilon)y, \quad (28)$$

where,

$$q_n(x, \varepsilon) = q'_{n-1}(x, \varepsilon) + s_{n-1}(x, \varepsilon) + q_0(x, \varepsilon)q_{n-1}(x, \varepsilon), \quad (29a)$$

$$s_n(x, \varepsilon) = s'_{n-1}(x, \varepsilon) + s_0(x, \varepsilon)q_{n-1}(x, \varepsilon), \quad (29b)$$

by considering sufficiently large values of  $n$ , the termination condition reads

$$\alpha(x, \varepsilon) = \frac{s_n(x, \varepsilon)}{q_n(x, \varepsilon)} = \frac{s_{n-1}(x, \varepsilon)}{q_{n-1}(x, \varepsilon)}, \quad (30)$$

Then, Eq.(28) has a general solution

$$y(x, \varepsilon) = e^{\int^x \alpha(t, \varepsilon) dt} [C_1 + C_2 \int^x e^{\int^t (2\alpha(\tau, \varepsilon) + q_0(\tau, \varepsilon)) d\tau} dt], \quad (31)$$

where  $C_1$  and  $C_2$  are integration constants.

The quantization condition reads

$$\delta_n(x, \varepsilon) = q_n(x, \varepsilon)s_{n-1}(x, \varepsilon) - q_{n-1}(x, \varepsilon)s_n(x, \varepsilon). \quad (32)$$

If the differential equation is analytically solvable in terms of polynomial solution then the following condition should be satisfied

$$\delta_n(x, \varepsilon) = 0, \quad (33)$$

using the following,

$$\delta_1(x, \varepsilon) = q_1(x, \varepsilon)s_0(x, \varepsilon) - q_0(x, \varepsilon)s_1(x, \varepsilon) = 0 \quad (34)$$

Applying in Eq.(16), hence, if we assume that  $\varepsilon = \nu^2$ , then we have the following:

$$s_0 = \frac{\varepsilon}{x^2} - \frac{1-\delta}{x} - \lambda, \quad (35a)$$

$$q_0 = -\frac{2\zeta}{x} - \frac{\gamma}{x^2}, \quad (35b)$$

$$s_1 = -\frac{\gamma\varepsilon}{x^4} - \frac{2\varepsilon+2\zeta\varepsilon+\gamma(\delta-1)}{x^3} + \frac{1-\delta+\lambda\gamma-2\zeta(\delta-1)}{x^2} + \frac{2\zeta\lambda}{x}, \quad (35c)$$

$$q_1 = \frac{\gamma^2}{x^4} + \frac{2\gamma+4\zeta\gamma}{x^3} + \frac{\varepsilon+2\zeta+4\zeta^2}{x^2} + \frac{\delta-1}{x} - \lambda \quad (35d)$$

$$s_2 = \frac{\gamma^2\varepsilon}{x^6} + \frac{6\gamma\varepsilon+4\zeta\gamma+\gamma^2(\delta-1)}{x^5} + \frac{6\varepsilon+8\zeta\varepsilon+5\gamma(\delta-1)+\varepsilon^2-\lambda\gamma^2+4(\delta-1)\zeta\gamma+4\zeta^2\varepsilon}{x^4} + \frac{2(\delta-1)-4\gamma\lambda+6\zeta(\delta-1)-4\lambda\gamma\zeta+2\varepsilon(\delta-1)+4(\delta-1)\zeta^2}{x^3} + \frac{4\zeta\lambda+2\varepsilon\lambda+4\zeta^2\lambda-(\delta-1)^2}{x^2} + \frac{2\lambda(1-\delta)}{x} + \lambda^2, \quad (36)$$

and



$$q_2 = -\frac{\gamma^3}{x^6} - \frac{\gamma^2(6 + 2\zeta + 4\zeta^2)}{x^5} - \frac{6\gamma + 18\gamma\zeta + 2\gamma\varepsilon + 12\gamma\zeta^2}{x^4} - \frac{4\zeta + 12\zeta^2 + 4\zeta\varepsilon + 2\gamma(\delta-1) + 8\zeta^3}{x^3} - \frac{2(\delta-1) + 4\zeta(\delta-1)}{x^2} + \frac{4\zeta\lambda}{x} \quad (37)$$

From  $\delta_1 = 0$ , we obtain the following conditions

$$\lambda = 0, \quad \delta = 1, \quad (38a)$$

$$\varepsilon^2 - 2\zeta\varepsilon - \gamma(1 - \delta) = 0, \quad (38b)$$

$$\varepsilon = \frac{\gamma\lambda}{\delta-1}, \quad (38c)$$

$$\varepsilon = \frac{(1-\delta)^2}{2\lambda} - \zeta. \quad (38d)$$

For simplicity, we look for the first condition  $\delta = 1, \lambda = 0$ , then we obtain the following solution,

$$\delta_1(x, \varepsilon) = \frac{\varepsilon(\varepsilon-2\zeta)}{x^4}, \quad (39a)$$

$$\delta_2(x, \varepsilon) = \frac{\varepsilon(\varepsilon-2\zeta)(2+4\zeta-\varepsilon)}{x^6}, \quad (39b)$$

$$\delta_3(x, \varepsilon) = -\frac{\varepsilon(\varepsilon-2\zeta)(2+4\zeta-\varepsilon)(6+6\zeta-\varepsilon)}{x^8}, \quad (39c)$$

Then, we can obtain  $\delta_n$  as follows:

$$\delta_n = \frac{(-1)^{n+1}}{x^{2n+1}} \prod_{r=0}^n (\varepsilon - r(2\zeta + r - 1)). \quad (40)$$

If we apply the quantization condition (Eq.(33)), AIM iteratively yields

$$\varepsilon = n(n + 2\zeta - 1), \quad n = 0, 1, 2, 3, \dots \quad (41)$$

Then, the corresponding eigenfunctions read as follows

$$y_0(x) = 1, \quad (42a)$$

$$y_1(x) = 2\zeta x + \gamma, \quad (42b)$$

$$y_2(x) = (2\zeta + 1)(2\zeta + 2)x^2 + 2(2\zeta + 1)\gamma x + \gamma^2, \quad (42c)$$

$$y_3(x) = (2\zeta + 2)(\zeta + 3)(\zeta + 4)x^3 + 3(2\zeta + 2)(2\zeta + 3)\gamma x^2 + 3(2\zeta + 2)\gamma^2 x + \gamma^3, \quad (42d)$$

and so, consequently, the recursive solution for  $y_n(x)$  is given by

$$y_n(x) = (2\zeta + n - 1)(2\zeta + n)(2\zeta + n + 1)x^n + \dots + \gamma^n. \quad (43)$$

## V. EIGENVALUES APPROXIMATIONS

### 1.5 Eigenvalue spectrum via AIM

The idea is to expand  $\delta_n(x, \varepsilon)$  by using Taylor's series at  $\varepsilon = 0$  for  $\delta_n(x, \varepsilon)$ , we obtain

$$\delta_n(x, \varepsilon) = \sum_{r=0}^{\infty} \varepsilon^r \delta_n^{(r)}(x, \varepsilon), \quad (44)$$

where,

$$\delta_n^{(r)}(x, \varepsilon) = \frac{1}{r!} \frac{\partial^r \delta_n(x, \varepsilon)}{\partial \varepsilon^r}. \quad (45)$$

From the solution of the equation  $\delta^{(0)}(x, \varepsilon)|_{\varepsilon=0} = 0$ , gives us  $\lambda^{(0)}$  and  $\delta^{(1)}(x, \varepsilon)|_{\varepsilon=0}$  gives  $\lambda^{(1)}$ , the first correction term to the eigenvalue. Consequently, it is easily to conclude for  $\lambda^{(0)}$  the following

$$\lambda_1^{(0)} = 0, \quad \lambda_2^{(0)} = \frac{\varepsilon(\delta-1)}{\gamma}, \quad \lambda_3^{(0)} = \frac{(\delta-1)^2}{2(\zeta+\varepsilon)}, \quad (46)$$

This procedure allows us to find the coefficients of the eigenvalue expansion  $\lambda_n^{(1)}, \lambda_n^{(2)}, \dots$ . By using programming manipulation, plugging in the quantization condition represented by Eq.(33) and Eq.(45) and by using the iterative symbolic computations of Maple program, then we get the value of the coefficients of the eigenvalue expansion (omitted here for brevity due to their long forms).

Consequently, the eigenvalue can be represented by the expansion

$$\lambda_n(\varepsilon) = \lambda_n^{(0)} + \varepsilon \lambda_n^{(1)} + \varepsilon^2 \lambda_n^{(2)} + \varepsilon^3 \lambda_n^{(3)} + \dots \quad (47)$$

and the series can be obtained dependent on the order of Bessel function ( $\varepsilon = \nu^2$ ).

### 1.6 Perturbed approximation of eigenvalues

Using the perturbation method, we seek the first order expansion for the special case of the generalized Bessel equation under the conditions  $\zeta = \gamma = 0$  and  $\delta = 1$ , with the form

$$y'' + (\lambda + \varepsilon f(x))y = 0, \quad \varepsilon \ll 1, y(0) = 0, y(b) = 0, \quad (48)$$

Where,



$$y = y_0 + \varepsilon y_1 + \varepsilon^2 y_2 + \dots, \quad \lambda^n = \lambda_0 + \varepsilon \lambda_1 + \varepsilon^2 \lambda^2 + \dots \quad (49)$$

Then, we have

$$\lambda_n = \frac{n^2 \pi^2}{b^2} - \frac{\varepsilon}{\int_0^b \sin^2 \frac{n\pi}{b} x dx} \int_0^b f(x) \sin^2 \frac{n\pi}{b} x dx, \quad (50)$$

By substituting with the following:  $f(x) = -\frac{1}{x^2}$ ,  $\varepsilon = v^2$  and  $z = \frac{n\pi}{b} x$ , we get,

$$\lambda_n = \frac{n^2 \pi^2}{b^2} + \frac{2\pi n v^2}{b^2} \int_0^b \frac{\sin^2 z}{z^2} dz, \quad (51)$$

If we assumed the following new function

$$SSi(x) = \int \frac{\sin^2 x}{x^2} dx = Si(2x) - \frac{\sin^2 x}{x}, \quad (52)$$

where  $si(x)$  and  $ci(x)$  are sine and cosine integral respectively.

As shown in Fig.5, it is easily to deduce that  $SSi(x)$  function is bounded through the range

$$|SSi(x)| \lesssim 1.555. \quad (53)$$

Finally, we get the following relation for the spectrum if  $|v| < 1$ ,

$$\lambda = \frac{n^2 \pi^2}{b^2} + \frac{3\pi n v^2}{b^2}. \quad (54)$$

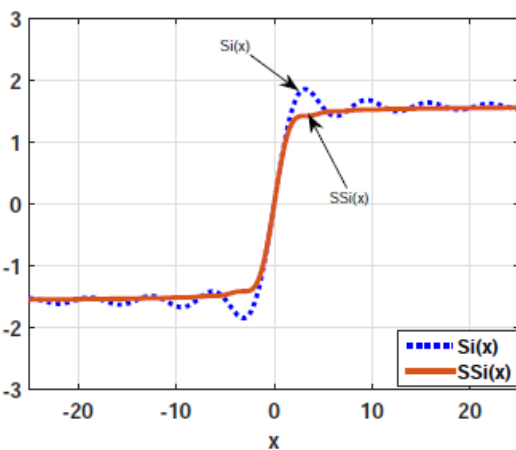


Figure 5. Graph of  $SSi(x)$  and  $Si(x)$  functions in  $[-25, 25]$ .

The total approximation of eigenvalue for the generalized Bessel equation can be obtained using approximation values of the parameters  $\delta$ ,  $\zeta$  and  $\nu$  in terms of  $v$ , when  $|v| \ll 1$ . However, by using the properties of Bessel, it might be obtained a series for  $\lambda_n$  in terms of the order and the boundary value  $b$ . Hence, let  $\xi_n, n=1,2,3,\dots$  be the positive

zeros of the  $J_\nu(x)$ ,  $\nu > 1$  using residue method for the following complex function,

$$f(z) = \frac{1}{z^2} \frac{J_\nu(z)}{J_\nu(z)} = \frac{\nu}{z^3} - \frac{1}{2(\nu+1)} \frac{1}{z} + O(z), \quad |z| \rightarrow 0, \quad (55)$$

The function  $f(z)$  has a pole at  $z = 0$  with residue  $(-\frac{1}{2(\nu+1)})$ . Also, the function  $f(z)$  has simple pole at  $z = \pm \xi_n$  with residue  $(\frac{1}{\xi_n})$ . Then, the following identity can be concluded,

$$\sum_{n=1}^{\infty} \left(\frac{1}{\xi_n}\right)^2 = \frac{1}{4(\nu+1)}, \quad (56)$$

Then, we obtain the following series for the eigenvalues,

$$\sum_{n=1}^{\infty} \frac{1}{\lambda_n} = \frac{1}{4b^2(\nu+1)}. \quad (57)$$

## VI. STABILITY CHART OF GENERALIZED BESSEL EQUATION

By using the approximation results of eigenvalues ( $\lambda$ ) with respect to the order ( $\nu$ ), the stability chart can be approximately anticipated between  $\lambda$  and  $\nu$ . It is approved numerically by using Fourier spectral method at  $\nu = 0$  on the interval  $(0, 2\pi)$  with boundary conditions  $y(0) = y(2\pi) = 0$ .

However, let us discuss the stability chart when  $\zeta = 0$  as shown in Fig.6. It is clearly shown that at  $\nu = 0$ , the fundamental eigenvalues are represented by  $\lambda = n^2$  if  $b = \pi$ , as a simple harmonic problem. Regarding the case of no damping, the characteristic equation represented by Eq.(54) which has a linear and parabolic behavior in  $\nu$  and whose solutions give curves  $\lambda = \lambda(\nu)$ . Setting  $\nu = 0$ , the intersection points in the  $\lambda$  axis can be obtained at the squared integer numbers. However, in the case of small values of  $\nu < 1$ , the curves has a parabolic shape coinciding with the analytical result. But for  $\nu > 1$  the linearized behavior is roughly seen. So that, with the aid of shifted spectral Fourier method, the numerical and analytical results are coincided.

Hereafter, for all values of  $\nu$ , the curves has two branches emitted from the axis  $\nu = 0$ , alike the stability chart of Mathieu equation. These curves are of even cosines and even sines at the even numbers and so odd cosines and odd sines at the odd numbers.

At every integer number, the emitted first curve represents the cosine solution and the second one represents the sine solution. The reason might go to the trigonometric structure of Bessel functions. Therefore, the behavior of the curves in the shown chart is explained in terms of cosines and sines functions.

Regarding the damping case, the effect of the damping term  $\zeta$  on the shape of the transition curves is to detach each

of the tongues from the  $\lambda$  axis. Thereby there exists a minimum value of  $\nu$  for instability to occur. Typically, as shown, the cosine branches represented by the dashed lines and the sine branches represented by the solid lines. Analogous to stability chart of Mathieu equation, the regions included by the two branches (the interior points inside the boundary curves) are the unstable domains but outside the branches, they are the stable domains.

Thus, they will be the domains of stability and the separating curves between the two regions are the transition curves of the Bessel equation. This clear that by checking the solutions at different points located in the unstable region, the boundary curves or the stable region. The influence of  $\zeta$  parameter on the stability chart is shown in Fig.7. It is clearly that, the increase of  $\zeta$  leads to move the minimum point to up producing the shrinkage of the unstable region.

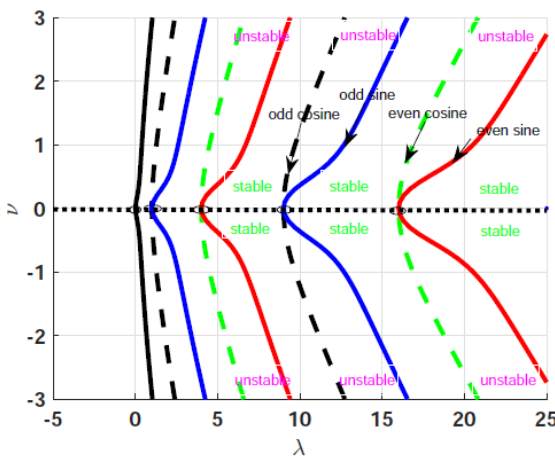


Figure 6. Stability chart of generalized Bessel equation

when  $\delta = 1$ , and  $\zeta = 0$ .

To take the influence of  $\delta$  on the stability chart of generalized Bessel equation (Eq.(16)) as shown in Fig.8, Fig.9 and Fig.10.

It is noted that, at the negative values of  $\delta$ , and around the value of  $\lambda = 0$ , there are disturbances in transition curves which means that the curves have non-uniformity in their behaviors due to the disturbance in the structure of trigonometric functions. When  $\delta \geq 0$  or going to be positive, the transition curves are going to be single boundary curves to separate the stability and instability regions as clearly shown for  $\delta = 0$  in Fig.9. At the larger values,  $\delta = 5$ , the transition curve at  $\zeta = 0$ , the sine and cosine curves are detached but for  $\zeta > 0$  the curves back to their standard shapes as shown in Fig.10.

For the validation of the results, the problem of periodic solutions with a specific period for Bessel equation may be formulated as an eigenvalue problem with the triple  $(\zeta, \lambda, \nu)$  in the interval  $[0, 2\pi]$  where  $h$  is mesh size in the

Fourier spectral method. To start the calculations, we will concern with the spectral methods which are a power tools for the computation of eigenvalues in different operators such as differential or integral operators. By considering that the problem is periodic, then it is used Fourier spectral method up to the second order differentiation matrix ( $D_M^{(1)}$  and  $D_M^{(2)}$ ,  $M = 250$ ). Then, it is looked for the periodic solutions in the stability chart in  $(\lambda, \nu)$  domain which represents the transition curves of the generalized Bessel equation.

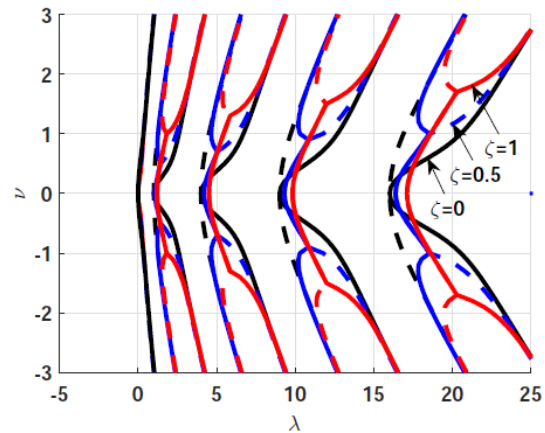


Figure 7. Stability chart of generalized Bessel equation

when  $\delta = 1$  at  $\zeta = 0, 0.5$  and  $1$ .

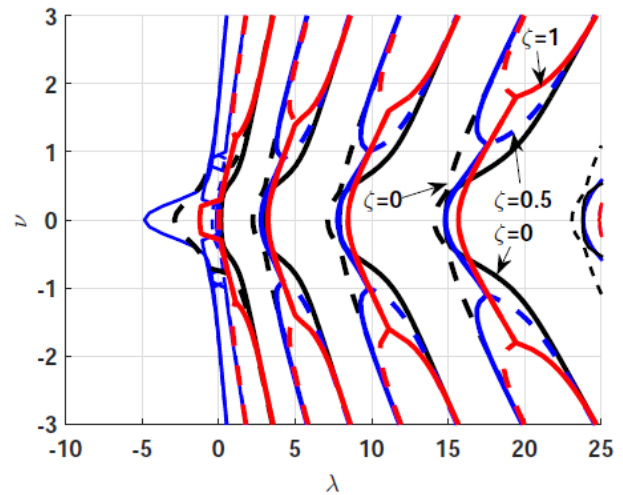


Figure 8. Stability chart of generalized Bessel equation when

$\delta = -1$  at  $\zeta = 0, 0.5$  and  $1$ .

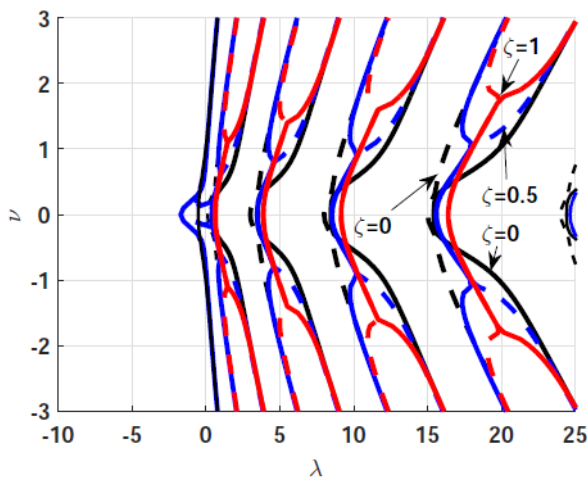


Figure 9. Stability chart of generalized Bessel equation when  $\delta = 0$  at  $\zeta = 0, 0.5$  and  $1$ .

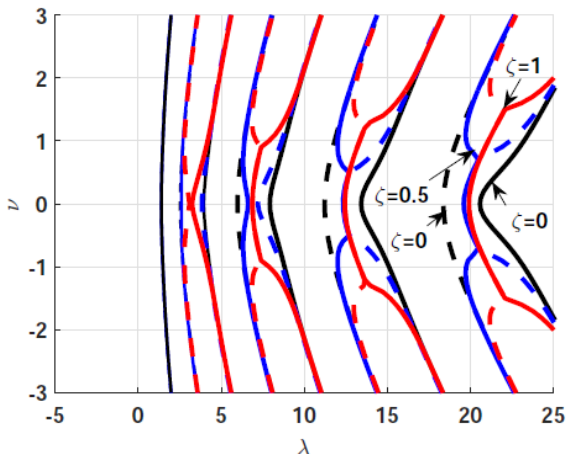


Figure 10. Stability chart of generalized Bessel equation when  $\delta = 5$  at  $\zeta = 0, 0.5$  and  $1$ .

## VII. CONCLUSION

Through the study of linear differential equations with periodic coefficients, a stability chart or Ince-Strutt diagram was generated to connect the eigenvalue parameter with the forcing amplitude. In such chart, the regions of stability and instability were clarified and separated by the eigenvalue curves (transition curves) to characterize by the presence of the periodic responses. In most dynamical systems with periodic coefficients, the determination of the semi-analytical relations of eigenvalue curves to graph the chart is based on angular Mathieu functions of first and second kinds. Some different examples are introduced and analyzed with their charts such as Mathieu equation, Ince equation and El Borhamy-Rashad- Sobhy equation.

Accordingly, it is suggested that the stability chart could be predicted and applied in linear differential equation with polynomial coefficients which possess a semi-periodic structure of solution such as generalized Bessel differential

equation. So that, due to the trigonometric structure of Bessel functions definitely at the integer order, the construction of stability chart and their transition curves has become a desirable and attractive thing via analytical or numerical methods.

The used analytical methods to obtain the characteristic equation were asymptotic approximation method for the generalized Bessel equation and the perturbation method for the undamped Bessel equation. The results are verified using shifted Fourier spectral method for certain cases with good agreement to each other. In general, the concluded result from this work may provide an insight into the prediction of stability charts for most linear differential equations with non-periodic coefficients, particularly that might have periodic structures of their solutions.

**Funding:** This work has not received any funding.

**Conflicts of Interest:** The author declares no competing interests.

## REFERENCES

- [1] Abuelma'atti, M.T., Trigonometric approximations for some Bessel functions. *Active and Passive Elect. Comp*, 22:75–85, 1999.
- [2] Abul-Ez, M., Zayed, M., and Youssef, A., Further developments of Bessel functions via conformable Calculus with applications. *Journal of Function Spaces*, 2021:ID 6069201, 1-17, 2021.
- [3] Baricz, A., *Generalized Bessel functions of the first kind*. Springer, 2010.
- [4] Bessel, F.W., *Untersuchung des Theils der planetarischen Störungen, welcher aus der Bewegung der Sonne entsteht*. Berliner Abh., 1–52, 1824.
- [5] Blachman, N.M. and Mousavinezhad, S.H., Trigonometric approximations for Bessel functions. *IEEE Transactions on Aerospace and Electronic systems*, AES 22(1):1–7, 1986.
- [6] Boyd, J.P., *Chebyshev and Fourier Spectral Methods*. 2nd ed., DOVER Publications, Inc., New York, 2000.
- [7] Brauer, F., On the Asymptotic Behavior of Bessel Functions. *Mathematical Association of America*, 70(9):954–957, 1963.
- [8] Brimacombe, C., Corless, R.M., and Zamir, M., *Computation and Applications of Mathieu Functions: A Historical Perspective*. *SIAM Review*, 63(4):653–720, 2021.
- [9] Butikov, E.I., Analytical expressions for stability regions in the Ince-Strutt diagram of Mathieu equation. *Am. J. Phys.*, 86(4):257–267, 2018.
- [10] Chert, L.Q. and Shen, J., Applications of semi-implicit Fourier spectral method to phase field equations. *Computer Physics Communications*, 108:147–158, 1998.
- [11] Chicone, C., *Ordinary differential equations with applications*. Springer, 2000. ISBN-10: 0-387-30769-9.
- [12] Coddington, E.A., and Levinson, N., *Theory of ordinary differential equations*. McGraw Hill, New York, 1955.
- [13] Cordero-Soto, R., and Suslov, S., The degenerate parametric oscillator and Ince's equation. *J. Phys. A: Math. Theor.*, 44:015101(1–10), 2010.
- [14] Cosson, R., Vermizzi, G., and Yang, X., *Mathieu functions and numerical solutions of the Mathieu equation*. *IEEE International Workshop on Open-source Software for Scientific Computation (OSSC)*, Guiyang, doi: 10.1109/OSSC.2009.5416839:3–10, 2009.
- [15] Cuyt, A., Lee, W., and Wu, M., High accuracy trigonometric approximations of the real Bessel functions of the first kind.

- Computational Mathematics and Mathematical Physics, 60(1):119–127, 2020.
- [16] Dehestani, H., Ordokhani, Y., and Razzaghi, M., Fractional order Bessel functions with various applications. *Applications of Mathematics*, 64(6):637–662, 2019.
- [17] Doha, E.H., Bhrawy, A.H., and Ezz-Eldien, S.S., A Chebyshev spectral method based on operational matrix for initial and boundary value problems of fractional order. *Computers and Mathematics with Applications*, 62:2364–2373, 2011.
- [18] El-Borhamy, M., El-Sheikh, Z., and Ali, M.E., Modeling and dynamic analysis for a motion of mounted-based axisymmetric rigid body under self-excited vibrations in an attractive Newtonian field. *Mathematical Problems in Engineering*, 2022: ID 4329906, 2022.
- [19] El-Borhamy, M., Rashad, E.M., and Sobhy, I., Floquet analysis of linear dynamic RLC circuits. *Open Physics*, 18:264–277, 2020.
- [20] El-Borhamy, M., Rashad, E.M., Nasef, A.A., Sobhy, I., and Elkholy, S.M., On the construction of stable periodic solutions for the dynamical motion of AC machines. *AIMS-Mathematics*, 8(4):8902–8927, 2023.
- [21] El-Borhamy, M., Rashad, E.M., Sobhy, I., and El-sayed, M., Modeling and semi-analytic stability analysis for dynamics of AC machines. *Mathematics*, 9:644(1–13), 2021.
- [22] Ganguli, R., Mandal, A.K., and Chowdhary, A.K., Stability of damped Mathieu equation. *I.E.E. - I.E.R.E. Proceedings- India*, 210–212, 1971.
- [23] Ince, E.L., A linear differential equations with periodic coefficients. *Proc. London Math. Soc.*, 23:56–74, 1923.
- [24] Infeld, E., Stability criteria for generalized Mathieu equations. *Quarterly of Applied Mathematics*, 301–304, 1976.
- [25] Insperger, T., and Stepa'n, G., Stability with the damped Mathieu equation with time delay. *J. Dynamic Systems, Measurement and Control*, 125:166–171, 2003.
- [26] Khosravian-Arab, H., Dehghan, M., and Eslahchi, M.R., Generalized Bessel's functions: Theory and thier applications. *Math Meth Appl Sci.*, 1–22, 2017.
- [27] Korenev, B.G., *Bessel functions and thier applications*. Taylor & Francis, New York, 2002.
- [28] Kurup, D.G., and Koithyar, A., New expansions of Bessel functions of first kind and complex argument. *IEEE Transations on Antennas and Propagation*, 61(5):2708–2713, 2013.
- [29] Mathieu, E', Mémoire sur le mouvement vibratoire d'une membrane de forme elliptique. *J. de mathématiques pures et appliquées*, 13:137–203, 1868.
- [30] McLachlan, N.W., *Theory and application of Mathieu functions*. Oxford University Press, 1951.
- [31] Merkin, D.R., *Introduction to the theory of stability*. Springer-Verlag, New York, 1997.
- [32] Narendra, K.S., and Taylor, J.H., Stability of the damped Mathieu equation. *IEEE Trans.*, AC-13:726–727, 1968.
- [33] Orel, B., and Perne, A., Chebyshev-Fourier spectral methods for nonperiodic boundary value problems. *Journal of Applied Mathematics*, 2014, ID 572694:1–10, 2014.
- [34] Parkas, P.C., Circle criterion and the damped Mathieu equation. *Electronic Letters*, 2(8):315, 1966.
- [35] Parra-Hinojosa, A., and Gutierrez-Vega, J.C., Fractional Ince equation with a Riemann-Liouville fractional derivative. *Applied Mathematics and Computation*, 219:10695–10705, 2013.
- [36] Pedersen, P., Stability of the solutions to Mathieu-Hill equations with damping. *Ingenieur-Archiv*, 49:15–29, 1980.
- [37] Pritchard, A.J., Stability of the damped Mathieu equation. *Electronic Letters*, 5(26):700–701, 1969.
- [38] Purser, F., Some applications of Bessel's functions to physics. *Proceedings of the Royal Irish Academy*, 26:25–66, 1907.
- [39] Rand, R.H., On the stability of Hill's equation with four independent parameters. *Journal of Applied Mechanics*, 885–886, 1969.
- [40] Rand, R.H., Sah, S.M., and Suchorsky, M.K., Fractional Mathieu equation. *Commun. Nonlinear Sci. Numer. Simulat.*, 15:3254–3262, 2010.
- [41] Ruby, L., Applications of the Mathieu equation. *Am. J. Phys.*, 64(1):39–44, 1996.
- [42] Taylor, J.H., and Narendra, K.S., Stability regions for the damped Mathieu equation. *Siam J. Appl. Math.*, 17(2):1–10, 1969.
- [43] Temme, N.M., *Special functions : an introduction to the classical functions of mathematical physics*. John Wiley & Sons, Inc., USA, 1996.
- [44] Watson, G.N., *A treatise on the theory of Bessel functions*. Cambridge university Press, 1995.
- [45] Webster, R.J., Formulas which approximate the distribution of a sinusoid plus noise. *IEEE Transactions on Information Theory*, IT-29(5):765–767, 1983.
- [46] Wilson, H.K., *Ordinary differential equations*. Edwards-vill, III, 1970.